ArvinMed International

Journal of Nanomedicine, Nanoscience and Technology

JNNT

Research Article

Amer MS, et al. Nanom Nanos Tech : JNNT : 109

Compressive Mechanical Behavior of Highly-Aligned Monolayer Films of Single-Walled Carbon Nanotubes Using Langmuir-Blodgett Technique

Maher S. Amer*, Ali M. Al Mafarage, Mohammed K. Mohammed

Department of Mechanical and Materials Engineering, Wright State University, Dayton, OH 45435, USA

***Corresponding author:** Maher S. Amer, Department of Mechanical and Materials Engineering, Wright State University, Dayton, OH 45435, USA. Email: maher.amer@wright.edu

Citation: Amer MS, Mafarage AMA, Mohammed MK (2019) Compressive Mechanical Behavior of Highly-Aligned Monolayer Films of Single-Walled Carbon Nanotubes Using Langmuir-Blodgett Technique. J Nanom Nanos Tech: JNNT-109.

Received Date: 20th February, 2019; **Accepted Date:** 28 February, 2019; **Published Date:** 08 March, 2019

Abstract

A truly single layer film of unmodified single-walled carbon nanotubes using the Langmuir-Blodgett (LB) technique have been processed for the first-time with measured compressive stress-strain behavior. The films were highly oriented as determined by polarized Raman spectroscopy and shown by scanning tunneling microscopy (STM). The films demonstrate a linear stress/strain behavior up to 30% strain and then deviate from linearity in a stress stiffening fashion. Maximum strain recorded was 50% without a sign of film collapse. The films exhibit a low compressive stiffness of 10±1 MPa. Electrical conductivity measurements of the films in both tube axial and transverse direction showed a difference in the range of five times higher in the axial direction with values of 4.8×10⁴ S/cm, and 1×10⁴ S/cm in the transverse directions, respectively.

Abstract

A truly single layer film of unmodified single-walled carbon nanotubes using the Langmuir-Blodgett (LB) technique have been processed for the first-time with measured compressive stress-strain behavior. The films were highly oriented as determined by polarized Raman spectroscopy and shown by scanning tunneling microscopy (STM). The films demonstrate a linear stress/strain behavior up to 30% strain and then deviate from linearity in a stress stiffening fashion. Maximum strain recorded was 50% without a sign of film collapse. The films exhibit a low compressive stiffness of 10±1 MPa. Electrical conductivity measurements of the films in both tube axial and transverse direction showed a difference in the range of five times higher in the axial direction with values of 4.8×10⁴ S/cm, and 1×10⁴ S/cm in the transverse directions, respectively.

Keywords: carbon nanotube, Langmuir-Blodgett film, Mechanical Properties, Raman spectroscopy, Electrical conductivity.

Introduction

Since their discovery in early 90s of last century, carbon nanotubes have created gigantic movement in many areas of science and engineering due to their remarkable mechanical, thermal, and electrical properties [1-3]. Specifically, this blend of properties makes them perfect as reinforcement in a new generation of multi-functional composite materials with engineered properties [4-7]. The realization of such advanced applications for carbon nanotubes, however, necessitates the development of processing techniques capable of manipulating and controlling the morphology of such nanotubes within the composite structure [2, 8-10]. While many investigations incorporated randomly oriented nanotubes in a polymer matrix using simple mixing techniques, other studies depended on growing nanotubes in a specific orientation and then incorporate the polymer matrix as a technique to control nanotubes' orientation within the composite [9, 11, 12]. The Langmuir-Blodgett technique with its ability to process highly oriented single-walled carbon nanotubes (SWCNTs) films drew attention and triggered several investigations [13-25]. Very few of such investigations, however, provided evidence for the true alignment of the produced films, and none provided evidence for the mono-layer nature of the films. For example, while Li, X. et al. [13], reported a Langmuir–Blodgett (LB) method achieving monolayers of aligned SWNTs with dense packing. They, in fact, did not provide any experimental evidence of film thickness or orientation. Others, however, reported LB processed SWCNT films with thicknesses ranging between 58 and 140 layers [20, 22, 25]. This is understood in the light of the fact that all the SWCNTs used in the aforementioned studies were not sorted or well-characterized.

In this paper, we report, for the first time, the production of true monolayer highly-aligned SWCNTs films by LB techniques without the need for the tubes surface oxidation, functionalization, or the use of compression/decompression cycles. Our currently produced films represent highly oriented, pure, unaltered SWCNTs films with all the superior properties of SWCNTs intact.

Experimental Procedure

We used purified Luna® single-walled carbon nanotubes (SWCNTs). The tubes were manufactured by Luna Technologies and are highly purified with less than 1 wt.% of metal catalyst remaining in them. Oversaturated solution of SWCNTs in dimethylformamide (DMF) solvent (Fisher Scientific, reagent grade) were sonicated in a 60 MHz ultrasonic bath (Fisher Scientific, Model FS20) for periods ranging between 30 minutes to 6.50 hours. The sonicated solution was then centrifuged (Beckman Coulter, Allegra™ X22R) for 30 minutes at 12000 RPM. The concentration of SWCNTs in pure centrifuged saturated solutions was measured using gravimetric method and was found to be 0.046 mg/mL based on 10 measurements using a balance with 0.1mN sensitivity as was described elsewhere [26]. Tubes were also characterized using high resolution transmission electron microscopy (HRTEM) (FEI, Themis Z).

Films were produced using a Langmuir-Blodgett (LB) trough (Nima Technology UK, 1222D2). Pure distilled water was used as a substrate for film deposition. Isotherms for the water subphase were run several times to ensure that the water surface is extremely clean. (Figure 1) shows a schematic describing the LB film production process. Our Langmuir-Blodgett trough is enclosed in a class 100 level clean enclosure (Nima Technology UK, 1222D2). 1000 µL of centrifuged SWCNTs in DMF solutions were spread on the subphase surface and left to evaporate the solvent for 30 minutes with an open trough area of 500 cm^2. Surface pressure/area isotherms were obtained at a barrier speed of 100 cm^2/min. All isotherms were repeated at least three times to ensure reproducibility of the results. All films in this study were deposited at a constant deposition pressure of 13.5 mN/m and vertical speed of the substrate of 5 mm/min. Deposition was achieved by starting the substrates under water surface and moving the substrate upwards to ensure high transfer rates. Film deposition was done on metal discs for further characterization by scanning tunneling microscope (STM) (NanoSurf easy Scan, E-Line). Films were also deposited on single crystal silicon wafers for further characterization using polarized Raman spectroscopy. Polarized Raman measurements (Reneshaw®, in Via Raman Microscope) were conducted using an Ar^+ laser at 514.5 nm wavelength as excitation light source in the back-scatter arrangement with a laser power of 2 mW at the sample surface to avoid sample heating. Both incident and scattered lights were polarized in the HH directions that is parallel to the nanotube alignment direction. The sample was mounted under the Raman microscope on a rotating stage and was rotated between 0º d 90º measured from the tube axial direction.

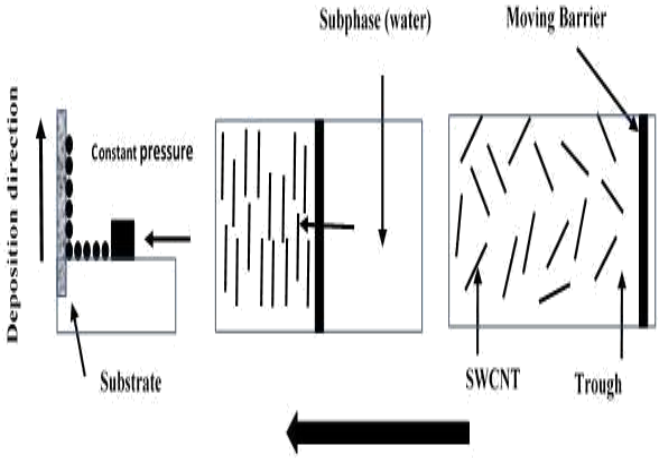

Figure 1: A schematic showing the Langmuir-Blodgett process.

Electric conductivity of the films was measured using a semiconductor parametric analyzer (Keithley 2041, Keithley Instruments Inc., Cleveland, OH) with 4-prob points method. This device can measure the voltage and current with a resolution of µV and pA, respectively.

Results and Discussions

Nanotubes characteristics

Figure 2 shows the radial breathing modes (RBM) region of the Raman spectrum for the Luna® SWCNTs used in this study after sonication and centrifuging. The RBM region of the spectrum shows three modes, at 106.85 cm^{-1}, 156.3 cm^{-1}, and 171.24 cm^{-1}, with integrated peak intensity (area under the peak) of 500, 9978, and 27300, respectively. Hence, based on the Raman integrated intensity of the peaks, our sample mainly consists of two types of nanotubes at a ratio of 27% and 73% respectively.

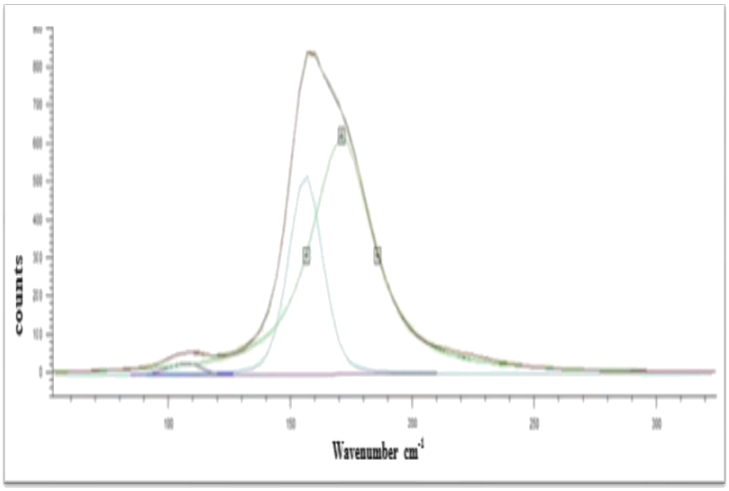

Figure 2: Radial breathing modes (RBM) region of the Raman spectrum. The RBM could be deconvoluted into 3 modes at 106.85 cm^{-1}, 156.3 cm^{-1}, and 171.24 cm^{-1}.

Utilizing the Raman position to determine the diameter of the nanotubes according to equation (1) [2, 27-29];

$$\nu(cm^{-1}) = \frac{223.75}{d(nm)} + 14 \qquad (1)$$

This shows that our sample consists of 27% of SWCNTs with diameter of 1.57 nm, and 73% of SWCNTs with a diameter of 1.42 nm. Nanotube diameters (*d*) were correlated to their chirality vector multiples (n, m) using the equation (2) [2];

$$d = \frac{a}{\pi}\sqrt{n^2 + nm + m^2} \qquad (2)$$

These diameter values were found to correspond to the metallic achiral (18,3), and the metallic zigzag (18,0) types of nanotubes. Since the majority (73%) of the nanotubes used in this investigation are (18,0), we will consider only the presence of such tubes in our sample in order to simplify the Langmuir-Blodgett isotherm calculations. In addition, the tubes were further characterized using high-resolution transmission electron microscopy (figure3).

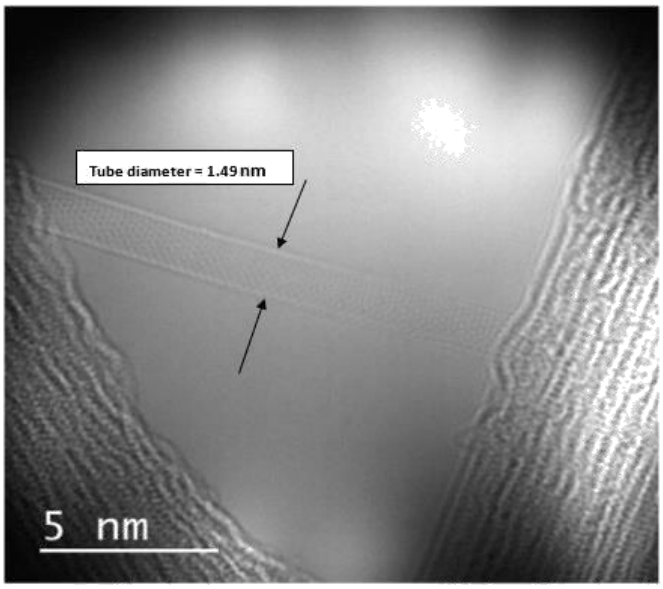

Figure 3: HRTEM image showing the characterization of a single wall carbon nanotube at the nano level.

The measured tube diameter was consistent with that deduced from Raman measurements. To this end, Raman and STM results are very clear and in agreement regarding the tube characterizations. The number of carbon atoms per unit cell was shown to be equal to 2N, and N for the (18,0) nanotubes can be calculated according to equation (3) [2];

$$N = \frac{2(n^2+nm+m^2)}{3d_H} \text{ since n-m=3qd}_H \qquad (3)$$

Where, dH is the highest common divisor of the coordinate multiples n, and m, that equals 6 in our case leading to 72 carbon atoms per unit cell of the (18,0) SWCNT. Hence the molecular weight of a unit cell of (18,0) SWCNT equals 864 g/mole. This value will enable us to calculate the number of unit cells added to the Langmuir-Blodgett trough and hence, calculate the area per unit cell of the formed SWCNT film as we will discuss in the following section.

The SWCNT unit cell length (T) can be determined from equation (4) [2];

$$T = \frac{a\sqrt{n^2+nm+m^2}}{\sqrt{3}\,d_H} \text{ since n-m=3qd}_H \qquad (4)$$

Where a = $|a_1| = 0.1421\sqrt{3} = 0.2461$ nm. For the (18,0) nanotubes, T equals 0.426 nm. Noting that the tube diameter should be increased by 0.337 nm to accommodate for the width of the electronic shell around the carbon skeleton, therefore, the trajectory area of a unit cell on the surface of the subphase surface should be T*(d+3.37) = 74.85 Å^2. This value will enable the calculations of the produced film thickness, hence produce the film's stress strain curve as we will discuss in the following section.

Langmuir-Blodgett Films

Figure 4 shows a typical LB isotherm with the solid phase region fitted to a linear equation to determine the solid phase film area at zero surface pressure [30-32].

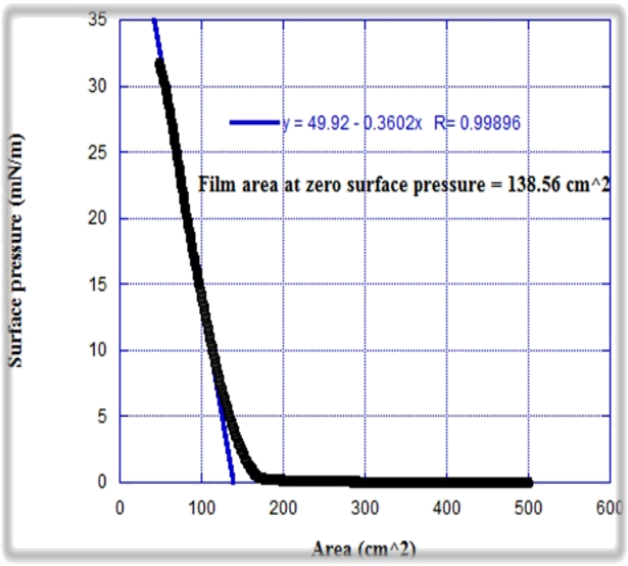

Figure 4: Langmuir-Blodgett isotherm with solid phase fitted for a linear equation for Film analysis.

Once the solid phase film area is determined at zero-applied surface pressure, the nondeformed dimensions of the solid phase film can be determined. Since the number of nanotube unit cells can be determined based on the weight of nanotubes added to the trough and the molecular weight of the individual unit cell, the number of unit cells added to the trough can be determined. In our study, 1000 µL of 0.046 mg/mL solution of (18,0) nanotubes would result in 3.2 E+16 unit-cells. If such a number of unit cells were to form a monolayer film, such film would have an area of 238.6 cm^2. From figure 4, the area of the nondeformed

solid state film (at zero surface pressure) is determined as 138.56 cm^2 indicating that the isotherm shown in figure 4 represents a film that has on average 1.7 layers of nanotubes. Another method to determine the film thickness is to divide the film measured area over the number of unit cells added to the trough to determine the area per unit cell as shown in figure 5. It is crucial to note that in figure 5, the nondeformed area per unit cell in the film was found to be 75 $Å^2$ that is very close to the area of an (18,0) nanotube unit cell of 74.85 $Å^2$ as shown above. This indicates that the film shown in figure 5 is a true monolayer film of the SWCNTs with a thickness of 1.42 nm.

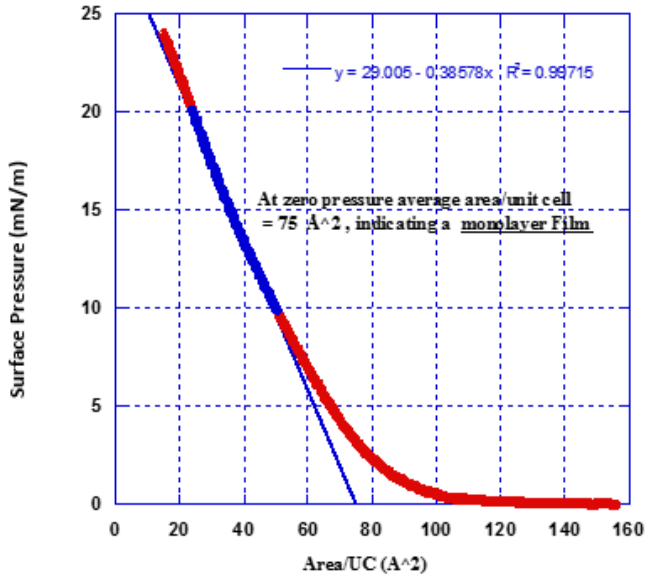

Figure 5: Langmuir-Blodgett isotherm for a monolayer film of SWCNT.

Stress-Strain curve of a monolayer SWCNT Films under compression

The process to calculate the film stiffness from the LB isotherm was discussed before [33, 34]. In brief, realizing that the width of the LB trough is constant (0.2 m in our study), the measured film area can be deduced to film length (L). Also, by considering a unit length along the film width, the measured surface pressure can be transformed into load (*F*). Knowing the film thickness, it is, then, straight forward to convert the load length curve into a stress-strain curve for the nano-film.

The stress-strain curve for the monolayer film is shown in figure 6. As shown in the figure, the stiffness of the film under compression is determined to be 10.2 ±1 MPa based on three different samples. Such low value of film stiffness compared to the well-known extremely high radial stiffness of SWCNTs [35-37] is not surprising. Noting that the film is very compliant with linear elastic behavior up to 30% strain, the film is basically behaving as a liquid crystal (LC) film of very stiff rods. Such similarity between nanotube films and liquid crystals (LC) was shown and discussed previously in the literature [26, 38, 39]. In addition, it is important to note the deviation from the linear behavior of the film under compression into a non-linear behavior with a clear stiffness increase (figure 6). Such behavior further supports the LC-like behavior of nano-films consisting of carbon nanotubes. Further investigation regarding the mechanical performance of such unique films are currently active in our research group.

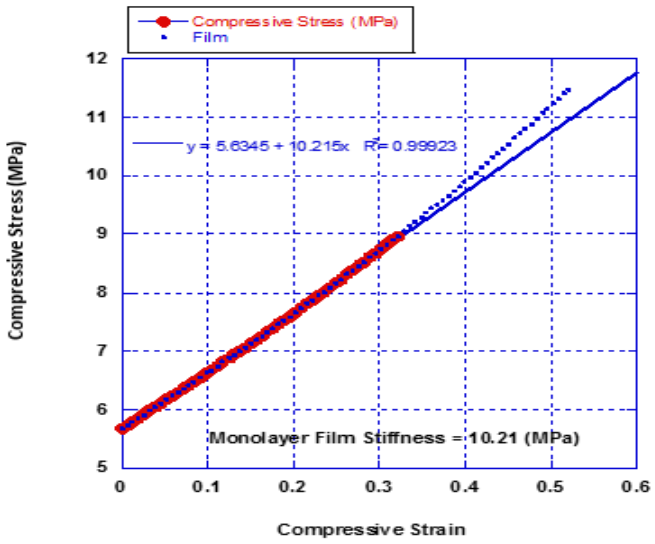

Figure 6: Stress/Strain curve for a monolayer SWCNT film in compression. Based on the LB isotherm shown in figure 5.

Nanotubes alignment within the film

Alignment of the SWCNTs within the processed films is expected to be achieved along the film width (normal to the film compression direction) due to the mechanics of the LB techniques. We investigated the nanotubes alignment within the film using both STM and polarized Raman spectroscopy. Figure 7 shows a 25×25 nm STM image for the monolayer film for which the LB isotherm is shown in figure 5. Once more, the image confirms the high level of alignment of SWCNTs within the monolayer film. Film alignment was further investigated using polarized Raman spectroscopy.

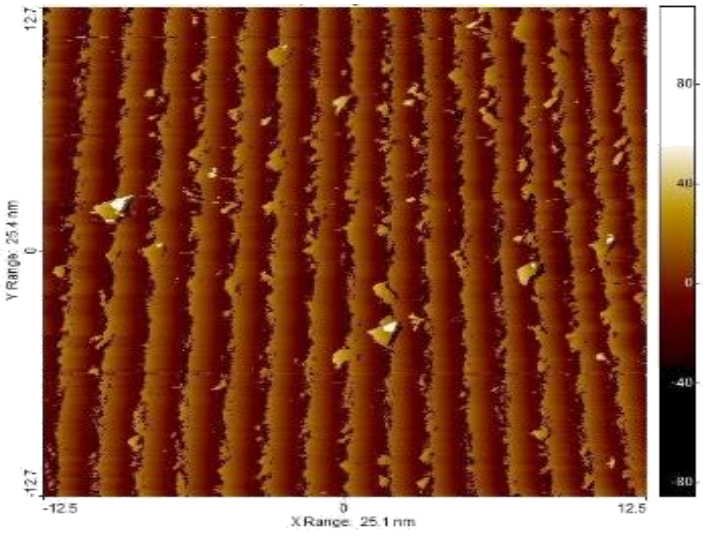

Figure 7: 25x25 nm STM image of a highly aligned monolayer film of SWCNTs.

Figure 8 shows Raman spectra obtained from our sample for the spectral range between 1125 cm^{-1} and 3200 cm^{-1} emphasizing the nanotube Raman active surface modes (D, G, and G' bands) [2, 40]. The spectra were collected in the HH back-scatter arrangement where both incident and scattered light are polarized in the same direction parallel to the tube orientation direction. The figure shows the spectra recorded at different angles between the polarization direction and the nanotubes orientation direction achieved in the LB trough. It is well known that in the HH backscattered Raman measurement arrangement, the intensity of the surface Raman modes depends on the orientation angle between the polarization and orientation directions [2, 41-43]. It is very clear from the polarized Raman results that our films are highly oriented as indicated by the total disappearance of all Raman surface active modes as the laser polarization direction is perpendicular to the nanotubes orientation direction.

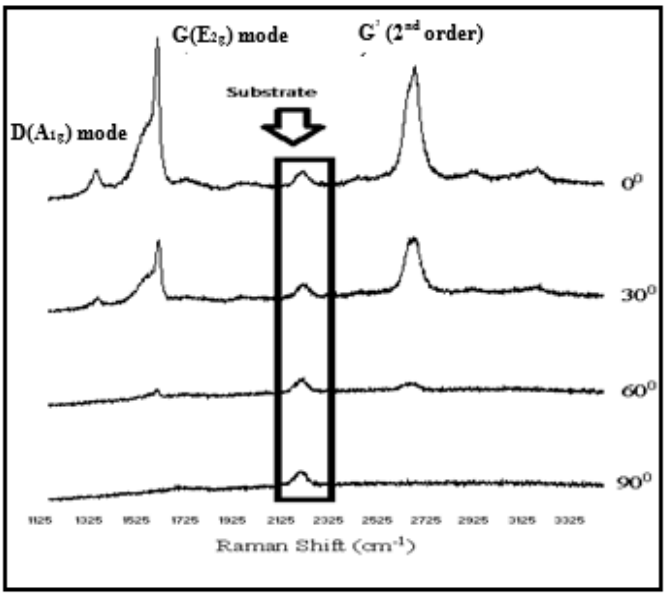

Figure 8: HH Polarized Raman spectra at different orientation angles between the SWCNT alignment angle and polarization angle. Spectra are showing First and second order NT surface modes. Spectra have been shifted for clarity. Note the persistent substrate Raman mode.

Figure 9 shows the measured electric conductivity of the film along as well as normal to that of the transverse conductivity of the film ($4.8x10^4$ vs. $1x10^4$ S/cm) which provides another evidence for the alignments of the tubes in the produced monolayer film. It is important to note that our measured electric conductivity of the film in the tube axial direction is slightly higher than the value $2.9x10^4$ S/cm reported previously for crystalline ropes of metallic SWCNTs that are 20 nm in diameter [44], and that our film conductivity measured in the transverse direction is slightly lower than the $1x10^4$ to $3x10^4$ S/cm reported for SWCNT networks [45].

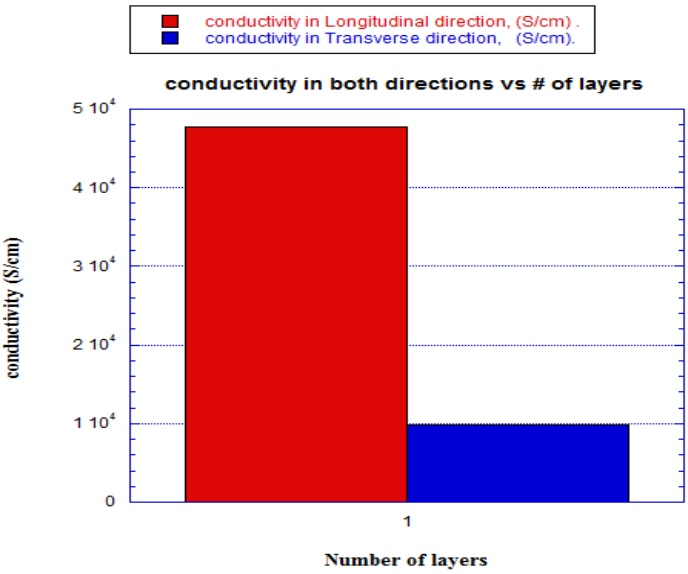

Figure 9: Histogram comparison for the conductivity (S/cm) in both directions for a monolayer film.

To this end, it is crucial to note that the processing of a single-layer unmodified SWCNT films would transform nanoelectronics device industry, it is also crucial, however, to note that such highly oriented films are extremely orthotropic with very different mechanical and electric properties in the tube axial and transverse directions. Attempts to deposit multiple layers at specific orientation to design a nano-film with specific properties in specific direction are currently under investigation in our research group.

Conclusions

In conclusion, we have shown that a mono-layer, highly oriented films of single-walled carbon nanotubes can be processed using the Langmuir-Blodgett technique. The compressive behavior of such highly orthotropic films demonstrated a linear stress/strain relationship up to 30% with an elastic modulus in the range of 10 MPa making its compressive behavior similar to rubbery materials. Our current study shows a processing methodology that would enable the full recognition of superior properties of nanotubes on a bulk scale.

Acknowledgements

Two of the authors, Ali M. Al Mafarage and Mohammed K. Mohammed, thankfully acknowledges the fellowship received from Higher Education Council of Iraq to pursue their Ph.D. Degree at Wright State University.

References

1. Endo M, Hayashi T, Ahm Kim Y, Terrones M, Dresselhaus MS (2004) "Applications of carbon nanotubes in the twentyâ €“first century," Philosophical Transactions of the Royal Society of London, Series A 362: 2223-2238.
2. Amer MS (2010) Raman Spectroscopy, Fullerenes, and Nanotechnology (Nanoscience and Nanotechnology, no. 13). Cambridge, UK: Royal Society of Chemistry: 290.

3. Cao J, Wang Q, Rolandi M, Dai H (2004) "Aharonov-Bohm Interference and Beating in Single-Walled Carbon-Nanotube Interferometers." Physical Review Letters 93: 216803.
4. Coleman JN, Khan U, Blau WJ, Gun'ko YK (2006) "Small but strong: A review of the mechanical properties of carbon nanotube–polymer composites." Carbon 44: 1624-1652.
5. Mazov IN, Ilinykha IA, Kuznetsov VL, Stepashkin AA, Ergin KS, et al. (2014) "Thermal conductivity of polypropylene-based composites with multiwall carbon nanotubes with different diameter and morphology," Journal of Alloys and Compounds 586: S440-S442.
6. Gibson RF (2010) "A review of recent research on mechanics of multifunctional composite materials and structures." Composite structures 92: 2793-2810.
7. Thostenson ET, Ren Z, Chou TW (2001) "Advances in the science and technology of carbon nanotubes and their composites: a review." Composites science and technology 61: 1899-1912.
8. Wenrong Yang, Liangti Qu, Rongkun Zheng, Zongwen Liu, Kyle R. Ratinac, et al. (2011) "Self-assembly of gold nanowires along carbon nanotubes for ultrahigh-aspect-ratio hybrids," Chemistry of Materials 23: 2760-2765.
9. Cebeci H, de Villoria RG, Hart AJ, Wardle BL (2009) "Multifunctional properties of high volume fraction aligned carbon nanotube polymer composites with controlled morphology." Composites Science and Technology 69: 2649-2656.
10. Qian H, Greenhalgh ES, Shaffer MSP, Bismarck A (2010) "Carbon nanotube-based hierarchical composites: a review," *Journal of Materials Chemistry,* 10.1039/C000041H 20: 4751-4762.
11. Vaddiraju S, Cebeci H, Gleason KK, Wardle BL (2009) "Hierarchical Multifunctional Composites by Conformally Coating Aligned Carbon Nanotube Arrays with Conducting Polymer." ACS Applied Materials & Interfaces 11: 2565-2572.
12. Tibbetts GG, Lake ML, Strong KL, Rice BP (2007) "A review of the fabrication and properties of vapor-grown carbon nanofiber/polymer composites." Composites Science and Technology 67: 1709-1718.
13. Xiaolin Li, Li Zhang, Xinran Wang, Iwao Shimoyama, Xiaoming Sun, et al. (2007) "Langmuir–Blodgett Assembly of Densely Aligned Single-Walled Carbon Nanotubes from Bulk Materials." Journal of the American Chemical Society 129: 4890-4891.
14. Kim Y, Minami N, Zhu W, Kazaoui S, Azumi R, ET AL. (2003) "Langmuir–Blodgett films of single-wall carbon nanotubes: layer-by-layer deposition and in-plane orientation of tubes." Japanese journal of applied physics 42: 7629, 2003.
15. Rodrigues RT, Morais PV, Nordi CSF, Schoning MJ, Siqueira JR, et al. (2018) "Carbon Nanotubes and Algal Polysaccharides to Enhance the Enzymatic Properties of Urease in Lipid Langmuir-Blodgett Films." (in English), Langmuir 34: 3082-3093.
16. Scholl FA, Morais PV, Gabriel RC, Schoning MJ, Siqueira JR, et al. (2017) "Carbon Nanotubes Arranged as Smart Interfaces in Lipid Langmuir-Blodgett Films Enhancing the Enzymatic Properties of Penicillinase for Biosensing Applications." (in English), Acs Applied Materials & Interfaces 9: 31054-31066.
17. Sun Q, Liu J, Chen M, Miyake J, Qian DJ (2014) "Fabrication and Characterization for the Nanoconjugates of Pyridyldithio-Functionalized Multiwalled Carbon Nanotubes and Cytochrome c in Langmuir-Blodgett Films." (in English), Journal of Nanoscience and Nanotechnology 14: 5468-5472.
18. Kaur R, Raina KK (2014) "Influence of single-wall carbon nanotubes on Langmuir-Blodgett films of ferroelectric liquid crystals as studied by atomic force microscopy." (in English), Liquid Crystals 41: 1065-1072.
19. Caseli L, Tiburcio VLB, Vargas FFR, Marangoni S, Siqueira JR (2012) "Enhanced Architecture of Lipid-Carbon Nanotubes as Langmuir-Blodgett Films to Investigate the Enzyme Activity of Phospholipases from Snake Venom." (in English), Journal of Physical Chemistry B 116: 13424-13429.
20. Massey MK, Pearson C, Zeze DA, Mendis BG, Petty MC (2011) "The electrical and optical properties of oriented Langmuir-Blodgett films of single-walled carbon nanotubes." Carbon 49: 2424-2430.
21. Simandan ID, Sava F, Velea A, Lorinczi A, Popescu M (2010) "Langmuir and Langmuir-Blodgett films based on stearic acid, barium stearate and carbon nanotubes." (in English), Optoelectronics and Advanced Materials-Rapid Communications 4: 1178-1181.
22. Gabriele Giancane, Andrés Ruland, Vito Sgobba, Daniela Manno, Antonio Serra, et al. (2010) "Aligning Single-Walled Carbon Nanotubes By Means Of Langmuir-Blodgett Film Deposition: Optical, Morphological, and Photo-electrochemical Studies," (in English), Advanced Functional Materials 20: 2481-2488.
23. Giancane G, Bettini S, Valli L (2010) "State of art in the preparation, characterisation and applications of Langmuir-Blodgett films of carbon nanotubes." (in English), Colloids and Surfaces a-Physicochemical and Engineering Aspects 354: 81-90.
24. Liu AR, Qian DJ, Wakayama T, Nakamura C, Miyake J (2006) "Monolayers, Langmuir-Blodgett films of carbon nanotubes-cytochrome c conjugates and electrochemistry." (in English), Colloids and Surfaces a-Physicochemical and Engineering Aspects 284: 485-489.
25. Yeji K, Nobutsugu M, Weihong Z, Said K, Reiko A, Mutsuyoshi M (2003) "Langmuir–Blodgett Films of Single-Wall Carbon Nanotubes: Layer-by-layer Deposition and In-plane Orientation of Tubes." Japanese Journal of Applied Physics 42: 7629, 2003.
26. Amer MS, Busbee JD (2011) "Self-Assembled Hierarchical Structure of Fullerene Building Blocks; Single-Walled Carbon Nanotubes and C60." The Journal of Physical Chemistry C 115: 10483-10488.

27. Rao AM, Richter E, Bandow S, Chase B, Eklund PC, et al. (1997) "Diameter-Selective Raman Scattering from Vibrational Modes in Carbon Nanotubes." Science 5297: 187-191.
28. Williams KA, Tachibana M, Allen JL, Grigorian L, Chengd S-C, et al. (1999) "Single-wall carbon nanotubes from coal," Chemical Physics Letters 310: 31-37.
29. Telg H, Maultzsch J, Reich S, Hennrich F, Thomsen C (2004) "Chirality Distribution and Transition Energies of Carbon Nanotubes." Physical Review Letters 93: 177401.
30. Petty MC (1996) Langmuir-Blodgett Films: An Introduction. Cambridge University Press.
31. Ulman A (2013) An Introduction to Ultrathin Organic Films: From Langmuir--Blodgett to Self-- Assembly. Academic press.
32. Barlow WA (2013) Langmuir-Blodgett Films. Elsevier Science.
33. Maher SA, Hasanain BA (2018) "On the processing of monolayer C 60 fullerene films and their mechanical properties." Materials Research Express 5: 016407.
34. Talebi HA (2017) "Mechanical and Optoelectric Properties of Fullerene Langmuir-Blodegett Nano-films" MS, Mechanical and Materials Engineering, Wright State University.
35. Wang X, Yong ZZ, Li QW (2012) "Ultrastrong, Stiff and Multifunctional Carbon Nanotube Composites." Materials Research Letters 1: 19-25.
36. Li C, Chou T.-W (204) "Elastic properties of single-walled carbon nanotubes in transverse directions." Physical Review B 69: 073401.
37. Batra RC, Sears A (2007) "Uniform radial expansion/contraction of carbon nanotubes and their transverse elastic moduli." Modelling and Simulation in Materials Science and Engineering 15: 835.
38. Shaffer M, Windle A (1999) "Analogies between polymer solutions and carbon nanotube dispersions." Macromolecules 32: 6864-6866.
39. Song W, Kinloch IA, Windle AH (2003) "Nematic Liquid Crystallinity of Multiwall Carbon Nanotubes." Science 302: 1363.
40. Dresselhaus MS, Dresselhaus G, Eklund PC (1996) Science of Fullerences and Carbon Nanotubes. San Diego: Academic Press.
41. Dresselhaus MS, Dresselhaus G, Jorio A, Souza Filho AG, Saito R (2002) "Raman spectroscopy on isolated single wall carbon nanotubes." Carbon 40: 2043-2061.
42. Fantini C, Jorio A, Souza M, Strano M, Dresselhaus M, et al. (2004) "Optical Transition Energies for Carbon Nanotubes from Resonant Raman Spectroscopy: Environment and Temperature Effects." Physical Review Letters 93: 147406-147409.
43. Jishi RA, Venkataraman L, Dresselhaus MS, Dresselhaus G (1993) "Phonon modes in carbon nanotubules." Chemical Physics Letters 209: 77-82.
44. Thess A, Lee R, Nikolaev P, Dai H, Petit P, et al. (1996) "Crystalline Ropes of Metallic Carbon Nanotubes." Science (New York, N.Y.) 273: 483-487.
45. Nirmalraj PN, Lyons PE, De S, Coleman JN, Boland JJ (2009) "Electrical connectivity in single-walled carbon nanotube networks." Nano Letters 9: 3890-3895.